Coupled-Trajectory Quantum-Classical Approach to Electronic Decoherence in Nonadiabatic Processes

Seung Kyu Min,[1,2] Federica Agostini,[1] and E. K. U. Gross[1]
[1]*Max-Planck Institut für Mikrostrukturphysik, Weinberg 2, D-06120 Halle, Germany*
[2]*Department of Chemistry, School of Natural Science, Ulsan National Institute of Science and Technology (UNIST), Ulsan 689-798, Korea*

(Received 1 April 2015; published 10 August 2015)

We present a novel quantum-classical approach to nonadiabatic dynamics, deduced from the coupled electronic and nuclear equations in the framework of the exact factorization of the electron-nuclear wave function. The method is based on the quasiclassical interpretation of the nuclear wave function, whose phase is related to the classical momentum and whose density is represented in terms of classical trajectories. In this approximation, electronic decoherence is naturally induced as an effect of the coupling to the nuclei and correctly reproduces the expected quantum behavior. Moreover, the splitting of the nuclear wave packet is captured as a consequence of the correct approximation of the time-dependent potential of the theory. This new approach offers a clear improvement over Ehrenfest-like dynamics. The theoretical derivation presented in this Letter is supported by numerical results that are compared to quantum mechanical calculations.

DOI: 10.1103/PhysRevLett.115.073001 PACS numbers: 31.50.Gh, 31.15.xg

The theoretical description of phenomena such as vision [1], photosynthesis [2], photovoltaic processes [3], and proton-transfer and hydrogen storage [4] is among the most challenging problems in condensed matter physics and theoretical chemistry. The underlying quantum dynamics of electrons and nuclei exhibit a nonadiabatic character, meaning that it cannot be explained by employing the Born-Oppenheimer (BO) approximation. In this respect, the major challenge for theory resides in the explicit treatment of electronic excited-state dynamics coupled to the nuclear motion. While methods that retain quantum features of the nuclear dynamics [5] are the most accurate to address this problem, they cannot be applied to systems with hundreds, or even thousands, of atoms. Therefore, a treatment of nuclear dynamics in terms of (semi)classical trajectories [5–9] represents the most promising and numerically feasible approach for actual calculations. Despite the great effort that has been devoted over the years to the development of such methods, actual applications are still limited [10]. Well-known issues are connected to the lack of, or incorrect account for, decoherence and to the inability of reproducing the spatial splitting of a nuclear wave packet, as in Ehrenfest-like dynamics. In the study of electronic nonadiabatic processes, these problems can result in wrong predictions for quantum populations and in unphysical outcomes for the nuclear dynamics.

We have recently proposed a new formalism that can be employed to overcome the above issues, the so-called exact factorization of the electron-nuclear wave function [11]. In this framework, the full wave function is written as the product of a nuclear wave function and an electronic factor with a parametric dependence on the nuclear configuration. Coupled equations drive the dynamics of the two components of the wave function. In particular, a time-dependent Schrödinger equation (TDSE) describes the evolution of the nuclear wave function where the effect of the electrons, beyond BO, is accounted for in a *single*, time-dependent, potential. Compared to a formulation in terms of multiple static adiabatic (or BO) potential energy surfaces (PESs), the advantage of this formulation is evident: when the classical approximation is introduced, the force driving the nuclear evolution can be *uniquely* determined from the gradient of this time-dependent potential [12].

In previous work, we have (i) analyzed the features of the time-dependent potential [13] in the context of nonadiabatic proton-coupled electron transfer, in order to pinpoint the properties that need to be accounted for when introducing approximations, (ii) determined the suitability of the classical and quasiclassical treatment [14] of nuclear dynamics, in a situation where the electronic effect can be taken into account exactly, and (iii) derived an independent-trajectory (IT) mixed quantum-classical (MQC) algorithm [7,8] to solve the coupled electronic and nuclear equations (from the factorization) in a fully approximate way. In particular, the IT-MQC scheme has been obtained as the *lowest-order* approximation, in an expansion in powers of $\hbar$ of the nuclear wave function in the complex-phase representation. Further investigation [15] has shown, however, that corrections are required if the nuclei exhibit a quantum behavior related to a nonadiabatic event, e.g., the splitting of a nuclear wave packet after the passage through an avoided crossing.

The aim of this Letter is to go beyond the IT-MQC algorithm of Refs. [7,8]. We have derived a coupled-trajectory (CT) MQC algorithm able to reproduce the features of the time-dependent potential, by evolving an ensemble of classical trajectories to mimic the quantum

evolution of the nuclei. Electronic populations, decoherence, and spatial splitting of the nuclear wave packet are correctly reproduced when the new scheme is employed, as will be demonstrated below.

The exact factorization approach consists in writing the solution $\Psi(\underline{\mathbf{r}}, \underline{\underline{\mathbf{R}}}, t)$ of the TDSE $\hat{H}\Psi = i\hbar\partial_t\Psi$, as the single product $\Psi(\underline{\mathbf{r}}, \underline{\underline{\mathbf{R}}}, t) = \Phi_{\underline{\underline{\mathbf{R}}}}(\underline{\mathbf{r}}, t)\chi(\underline{\underline{\mathbf{R}}}, t)$, where $\Phi_{\underline{\underline{\mathbf{R}}}}(\underline{\mathbf{r}}, t)$ is an electronic factor parametrically depending on the nuclear positions and $\chi(\underline{\underline{\mathbf{R}}}, t)$ is a nuclear wave function. Here, $\hat{H} = \hat{T}_n + \hat{H}_{\mathrm{BO}}$ is the Hamiltonian describing the system of interacting electrons and nuclei, with $\hat{T}_n$ the nuclear kinetic energy and $\hat{H}_{\mathrm{BO}}$ the BO Hamiltonian containing all interactions among the particles and the electronic kinetic energy. The positions of N_e electrons and N_n nuclei are represented by the symbols $\underline{\mathbf{r}}$ and $\underline{\underline{\mathbf{R}}}$, respectively. The product form of Ψ is unique, up to within an $(\underline{\underline{\mathbf{R}}}, t)$-dependent gaugelike transformation, if the partial normalization condition $\int d\underline{\mathbf{r}}|\Phi_{\underline{\underline{\mathbf{R}}}}(\underline{\mathbf{r}}, t)|^2 = 1 \forall \underline{\underline{\mathbf{R}}}, t$ is imposed. The evolution of the two components of the full wave function is governed by an electronic equation

$$\{\hat{H}_{\mathrm{BO}} + \hat{U}_{en}[\Phi_{\underline{\underline{\mathbf{R}}}}, \chi] - \epsilon(\underline{\underline{\mathbf{R}}}, t)\}\Phi_{\underline{\underline{\mathbf{R}}}} = i\hbar\partial_t\Phi_{\underline{\underline{\mathbf{R}}}} \quad (1)$$

and a nuclear equation

$$\left[\sum_{\nu=1}^{N_n} \frac{[-i\hbar\nabla_\nu + \mathbf{A}_\nu(\underline{\underline{\mathbf{R}}}, t)]^2}{2M_\nu} + \epsilon(\underline{\underline{\mathbf{R}}}, t)\right]\chi = i\hbar\partial_t\chi, \quad (2)$$

which are exactly equivalent to the full TDSE. The electron-nuclear coupling operator

$$\begin{aligned}\hat{U}_{en}[\Phi_{\underline{\underline{\mathbf{R}}}}, \chi] = &\sum_{\nu=1}^{N_n} \frac{[-i\hbar\nabla_\nu - \mathbf{A}_\nu(\underline{\underline{\mathbf{R}}}, t)]^2}{2M_\nu} \\ &+ \frac{1}{M_\nu}\left(\frac{-i\hbar\nabla_\nu\chi}{\chi} + \mathbf{A}_\nu(\underline{\underline{\mathbf{R}}}, t)\right) \\ &\times [-i\hbar\nabla_\nu - \mathbf{A}_\nu(\underline{\underline{\mathbf{R}}}, t)] \end{aligned} \quad (3)$$

represents the effect of the nuclei on electronic dynamics; in turn, the time-dependent vector potential

$$\mathbf{A}_\nu(\underline{\underline{\mathbf{R}}}, t) = \langle\Phi_{\underline{\underline{\mathbf{R}}}}(t)| - i\hbar\nabla_\nu\Phi_{\underline{\underline{\mathbf{R}}}}(t)\rangle_{\underline{\mathbf{r}}} \quad (4)$$

and time-dependent PES (TDPES)

$$\epsilon(\underline{\underline{\mathbf{R}}}, t) = \langle\Phi_{\underline{\underline{\mathbf{R}}}}(t)|\hat{H}_{\mathrm{BO}} + \hat{U}_{en} - i\hbar\partial_t|\Phi_{\underline{\underline{\mathbf{R}}}}(t)\rangle_{\underline{\mathbf{r}}} \quad (5)$$

account for the electronic backreaction on the nuclei in a Schrödinger-like equation. These potentials are uniquely determined [11] up to within a gauge transformation.

The CT-MQC scheme adopts a description of nuclear dynamics in terms of classical trajectories, $\underline{\underline{\mathbf{R}}}^{(I)}(t)$; thus, all quantities depending on $\underline{\underline{\mathbf{R}}}, t$ will become functions of $\underline{\underline{\mathbf{R}}}^{(I)}(t), t$. Nuclear dynamics will be *sampled* by using trajectories, meaning that we track the evolution of a nuclear wave packet by looking at how the trajectories evolve in time. Information about the nuclear space $\underline{\underline{\mathbf{R}}}$ is available only at the instantaneous positions along the classical paths. It follows that we will not be able to calculate partial time derivatives, but only total time derivatives, by using the chain rule $d/dt = \partial_t + \sum_\nu \mathbf{V}_\nu^{(I)} \cdot \nabla_\nu$, with $\mathbf{V}_\nu^{(I)} = \dot{\mathbf{R}}_\nu^{(I)}(t)$ the nuclear velocity. Henceforth, the superscript (I) will be used to indicate a spatial dependence, e.g., $\mathbf{A}_\nu^{(I)}(t) = \mathbf{A}_\nu[\underline{\underline{\mathbf{R}}}^{(I)}(t), t]$.

The main steps in the derivation of the new CT-MQC scheme are the following: (a) We approximate the TDPES, to avoid expensive calculations of second-order derivatives of the electronic wave function with respect to the nuclear coordinates; (b) we fix the gauge freedom; (c) we introduce a quasiclassical interpretation of the nuclear wave function, whose phase is connected to the classical momentum and whose modulus is reconstructed in terms of Gaussian wave packets; (d) we expand the electronic wave function on the adiabatic basis (Born-Huang expansion), $\Phi^{(I)}(t) = \sum_l |C_l^{(I)}(t)| \exp[(i/\hbar)\gamma_l^{(I)}(t)]\varphi_l^{(I)}$; hence, a set of partial differential equations for the coefficients of the expansion will be coupled to the nuclear equation. Also the full wave function can be expanded on the adiabatic basis, with coefficients $F_l(\underline{\underline{\mathbf{R}}}, t)$, for the exact expression, or $F_l^{(I)}(t)$, for the quantum-classical case, and will be referred to as BO-projected wave packets.

(a) In the expression of the TDPES, we neglect the contribution of $\langle\Phi_{\underline{\underline{\mathbf{R}}}}(t)|\hat{U}_{en}|\Phi_{\underline{\underline{\mathbf{R}}}}(t)\rangle_{\underline{\mathbf{r}}}$. Notice that the expectation value on $\Phi_{\underline{\underline{\mathbf{R}}}}$ of the second and third line of Eq. (3) is zero by construction; thus, the neglected term in the expression of the TDPES contains the second-order variations of the electronic state with respect to the nuclear coordinates, which is small [16–18] compared to the first order. Therefore, the TDPES is approximated as the sum of the two remaining terms in Eq. (5), $\epsilon(\underline{\underline{\mathbf{R}}}, t) \simeq \epsilon_0(\underline{\underline{\mathbf{R}}}, t) + \epsilon_{\mathrm{TD}}(\underline{\underline{\mathbf{R}}}, t)$, and Eqs. (1) and (2) become

$$i\hbar\dot{\Phi}^{(I)} = \hat{H}_{\mathrm{BO}}\Phi^{(I)} - \sum_{\nu=1}^{N_n} \frac{\mathcal{P}_\nu^{(I)}}{M_\nu} \cdot (\mathbf{A}_\nu^{(I)} + i\hbar\nabla_\nu)\Phi^{(I)} \quad (6)$$

and

$$\begin{aligned}\mathbf{F}_\nu^{(I)} = &-\langle\Phi^{(I)}|(\nabla_\nu\hat{H}_{\mathrm{BO}})|\Phi^{(I)}\rangle_{\underline{\mathbf{r}}} \\ &+ \sum_{\nu'=1}^{N_n} \frac{2i\mathcal{P}_{\nu'}^{(I)}}{\hbar M_{\nu'}}(A_{\nu'}^{(I)}A_\nu^{(I)} - \hbar^2\Re\langle\nabla_{\nu'}\Phi^{(I)}|\nabla_\nu\Phi^{(I)}\rangle_{\underline{\mathbf{r}}}),\end{aligned} \quad (7)$$

respectively, where the symbol $\dot{\Phi}^{(I)}$ is used to indicate the full time derivative of the electronic wave function and $\mathcal{P}_\nu^{(I)}$ will be specified below. The equations have been cast in such a way that the first terms on the right-hand side are exactly the same as in the Ehrenfest scheme [19]. The additional terms are corrections, whose effect will be now investigated.

(b) In deriving these expressions for the evolution of the electronic wave function, Eq. (6), and for the classical nuclear force, Eq. (7), the gauge freedom has been fixed by imposing $\epsilon_0^{(I)}(t) + \epsilon_{\mathrm{TD}}^{(I)}(t) + \sum_\nu \mathbf{V}_\nu^{(I)} \cdot \mathbf{A}_\nu^{(I)}(t) = 0$.

(c) The corrections beyond Ehrenfest in Eqs. (6) and (7) contain a term $\boldsymbol{\mathcal{P}}_\nu^{(I)}(t) = -i\hbar\nabla_\nu|\chi^{(I)}(t)|/|\chi^{(I)}(t)|$, which we will refer to as *quantum momentum*. The reason for this choice lies in the following expression:

$$\frac{-i\hbar\nabla_\nu\chi(\underline{\underline{\mathbf{R}}},t)}{\chi(\underline{\underline{\mathbf{R}}},t)} + \mathbf{A}_\nu(\underline{\underline{\mathbf{R}}},t) \simeq \mathbf{P}_\nu^{(I)}(t) + \boldsymbol{\mathcal{P}}_\nu^{(I)}(t) \quad (8)$$

for the term in Eq. (3) that explicitly depends on the nuclear wave function. Such a term has to be approximated when a trajectory-based treatment is adopted. In fact, Eq. (8) has been obtained by writing the nuclear wave function in polar form, $\chi = |\chi|e^{iS/\hbar}$, and then identifying (quasiclassically) $\nabla_\nu S + \mathbf{A}_\nu = \mathbf{P}_\nu$, with $\mathbf{P}_\nu$ the classical nuclear momentum and $\dot{\mathbf{P}}_\nu = \mathbf{F}_\nu$ from Eq. (7).

(d) If compared to the Ehrenfest scheme, the implementation of the CT-MQC algorithm based on Eqs. (6) and (7) requires only two additional steps: the calculation of (i) $\nabla_\nu\Phi^{(I)}$ and (ii) $\boldsymbol{\mathcal{P}}_\nu^{(I)}$. We employ the Born-Huang expansion of $\Phi^{(I)}$, in order to express term (i) by using the derivatives of the expansion coefficients, indicated by the symbols $C_l^{(I)}(t)$, and the nonadiabatic coupling vectors. The approximation $\nabla_\nu C_l^{(I)} \simeq (i/\hbar)\nabla_\nu\gamma_l^{(I)}C_l^{(I)}$ used here, with $\gamma_l^{(I)}(t)$ the phase of $C_l^{(I)}(t)$, is consistent with previous analysis reported in Refs. [13,14]. Moreover, based on quasiclassical considerations described in detail in Supplemental Material [20], we further approximate $\nabla_\nu\gamma_l^{(I)}(t) \simeq -\int^t d\tau\nabla_\nu\epsilon_{\mathrm{BO}}^{(l),(I)}$. Term (ii) is calculated by assuming that the nuclear density is a combination of Gaussian-shaped wave packets, each corresponding to a given adiabatic state. Notice that this approximation is not used in general in the algorithm but only to estimate the quantum momentum. For a two-state model, $\boldsymbol{\mathcal{P}}_\nu^{(I)}$ becomes [15] a linear function in the region where $\rho_l^{(I)}(t) = |C_l^{(I)}(t)|^2 \neq 0, 1$, while it is set to zero elsewhere (see Supplemental Material [20] and the discussion below). The generalization of this approximation to multiple states is straightforward and will be presented elsewhere [22]. The parameters of such a linear function are the slope and the y intercept, where the former is determined analytically by using Gaussian-shaped nuclear wave packets and the latter is obtained by enforcing (the reasonably physical condition) that no population exchange occurs when the nonadiabatic coupling vectors are zero. Information about the positions of all trajectories at a given time is required when evaluating these two parameters, thus resulting in a procedure beyond the IT-MQC approach: the classical trajectories cannot be evolved independently from each other; they are *coupled*.

The major advantage of the CT-MQC scheme developed here is that this procedure naturally incorporates *decoherence* effects. In the following, we shall discuss this feature in detail. After the nuclear wave packet has left a region of strong nonadiabatic coupling, the population $\rho_l^{(I)}(t) = |C_l^{(I)}(t)|^2$ of the lth BO state changes in time as

$$\dot{\rho}_l^{(I)} = -\sum_{\nu=1}^{N_n} \frac{2i\boldsymbol{\mathcal{P}}_\nu^{(I)}}{\hbar M_\nu} \cdot (\mathbf{A}_\nu^{(I)} - \nabla_\nu\gamma_l^{(I)})\rho_l^{(I)}. \quad (9)$$

In this region, the expression of the vector potential reduces to $\mathbf{A}_\nu^{(I)}(t) = \sum_l \rho_l^{(I)}(t)\nabla_\nu\gamma_l^{(I)}(t)$, since the nonadiabatic coupling vectors are negligible. In Eq. (9), we observe that, once $\rho_l^{(I)}(t)$ has approached the values 0 or 1, the term on the right-hand side becomes zero; thus, the electronic population remains constant (to 0 or 1) $\forall l$. This is a clear indication of decoherence, since the (squared modulus of the) off-diagonal elements of the electronic density matrix, often used as a measure of electronic coherence, become zero. Therefore, the correction terms beyond Ehrenfest in Eqs. (6) and (7), proportional to the quantum momentum, will be referred to as *decoherence terms*. Obtaining this feature is a clear improvement over the Ehrenfest approach and, likewise, over the IT-MQC approach [7,8] deduced from the exact factorization. Decoherence naturally appears by including dominant corrections in the expression of the nuclear wave function, leading to the appearance of the quantum momentum.

Numerical results obtained by implementing the above-described method are shown below in comparison to exact calculations. We discuss the performance of the CT-MQC algorithm in comparison to Ehrenfest dynamics for a two-state problem [23] involving the passage of the nuclear wave packet through a single avoided crossing, case (1), and in comparison to trajectory surface hopping (TSH) for a two-state problem involving the reflection of the nuclear wave packet from a potential barrier and its consequent spatial splitting, case (2), commonly known as the Tully-3 model [9]. The computational details for these two problems are given in Supplemental Material [20].

The TDPES for model case (1) is shown in Fig. 1 (upper panels). It develops steps and the nuclear wave packet correctly splits at the avoided crossing (Fig. 1, lower panels). It is worth noting that Ehrenfest dynamics completely misses the splitting, as we have shown in Ref. [8]. Furthermore, despite the fact that Ehrenfest dynamics properly reproduces the populations of the electronic states, as shown in Fig. 3 (upper left panel), it does not capture decoherence. On the contrary, the CT-MQC procedure slightly underestimates the nonadiabatic population exchange but correctly reproduces decoherence (Fig. 3, lower left panel).

In Fig. 3, we have used the quantity $N_{\mathrm{traj}}^{-1}\sum_I \rho_1^{(I)}(t)\rho_2^{(I)}(t)$ as a measure of decoherence, whose quantum equivalent is $\int d\underline{\underline{\mathbf{R}}}\rho_1(\underline{\underline{\mathbf{R}}},t)\rho_2(\underline{\underline{\mathbf{R}}},t)|\chi(\underline{\underline{\mathbf{R}}},t)|^2$. Here, the nuclear density has been replaced by its "classical" approximation, i.e., $|\chi(\underline{\underline{\mathbf{R}}},t)|^2 \simeq N_{\mathrm{traj}}^{-1}\sum_I \delta[\underline{\mathbf{R}} - \underline{\mathbf{R}}^{(I)}(t)]$.

We show in Fig. 2 (lower panels) that the CT-MQC algorithm reproduces the splitting of the nuclear wave packet due to the reflection from the barrier. In fact, the

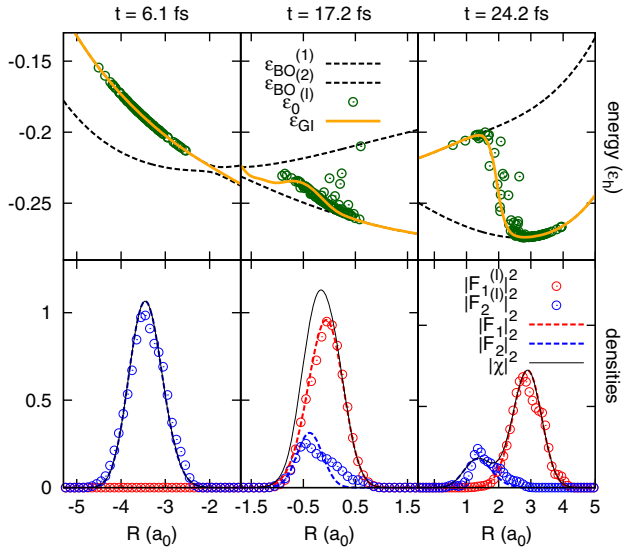

FIG. 1 (color online). Snapshots at different times for model case (1) of (top) the gauge-invariant (GI) part of the scalar potential $\epsilon_{\mathrm{GI}}(\underline{\underline{\mathbf{R}}},t)=\langle\Phi_{\underline{\underline{\mathbf{R}}}}(t)|\hat{H}_{\mathrm{BO}}+\hat{U}_{en}|\Phi_{\underline{\underline{\mathbf{R}}}}(t)\rangle_{\underline{\mathbf{r}}}$ (lines) compared to its approximation $\epsilon_0^{(I)}(t)$ (dots) used in the CT-MQC calculations, in Hartree ϵ_h (the BO surfaces are plotted for reference as dashed black lines); (bottom) nuclear density $|\chi(\underline{\underline{\mathbf{R}}},t)|^2$ (black line) and BO-projected densities (dashed lines) compared to the values of the BO-projected densities along the trajectories (dots).

TDPES develops the well-studied [13] steps (Fig. 2, upper panels) that bridge piecewise adiabatic shapes and allow trajectories in different regions of space to feel different forces. This feature is the strength of a procedure based on the exact factorization: a *single* time-dependent potential generating very different forces in different regions of space. It is known [9] that TSH as well is able to capture the reflection event for a low initial momentum of the nuclear wave packet but suffers from overcoherence [10,24]. In fact, as shown in Fig. 3, TSH completely misses decoherence,

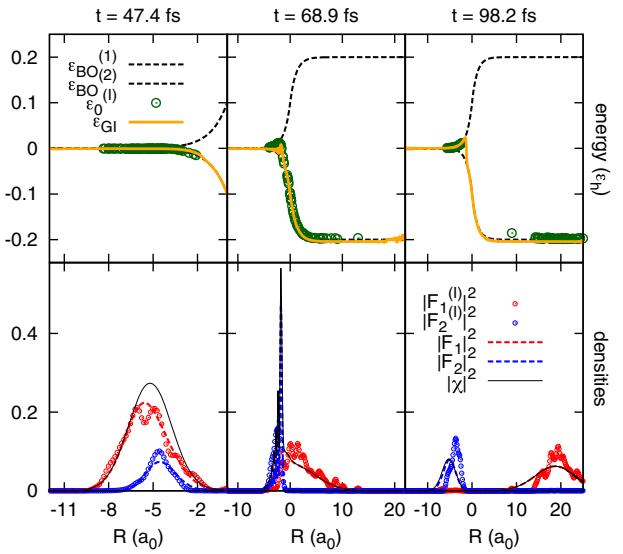

FIG. 2 (color online). The same as Fig. 1 for model case (2).

whereas the CT-MQC scheme not only reproduces the populations of the electronic states as functions of time (Fig. 3, upper right panel) but can also capture electronic decoherence (Fig. 3, lower right panel). The comparison between exact and CT-MQC results is overall remarkable and a clear step forward in comparison to other methods.

In this Letter, we have proposed a CT-MQC scheme based on the exact factorization formalism and tested it on a typical example of an electronic nonadiabatic process. The resulting equations give additional terms compared to Ehrenfest dynamics, that appear to be responsible for decoherence. The comparison of the CT-MQC scheme with full quantum mechanical results shows that we can correctly predict both electronic and nuclear properties: population dynamics, nuclear wave packet splitting, and decoherence. Nonadiabatic transitions are induced by the classical nuclear momentum, the zeroth order term of the $\hbar$ expansion of the nuclear wave function, and decoherence is the effect of the dominant corrections to the momentum. In addition, we have proven that, as discussed in our previous work [13,14], being able to catch the main features of the time-dependent potential in an approximate scheme results in the correct description of the nuclear dynamics. The major advantages of our CT-MQC algorithm over commonly used methods are (i) the working equations are conceptually and computationally as simple as Ehrenfest equations, and (ii) a small number of trajectories is required, because *only* initial conditions are to be sampled (no stochastic element is introduced). Working in the framework of the exact factorization allows us to systematically improve previous approximations, as we have shown in this Letter in comparison to the IT-MQC of Refs. [7,8]. Along similar lines, future work will focus on including quantum nuclear effects, such as interference, adopting a semiclassical representation of nuclear dynamics.

Partial support from the Deutsche Forschungsgemeinschaft (SFB 762) and from the European Commission (FP7-NMP-CRONOS) is gratefully acknowledged.

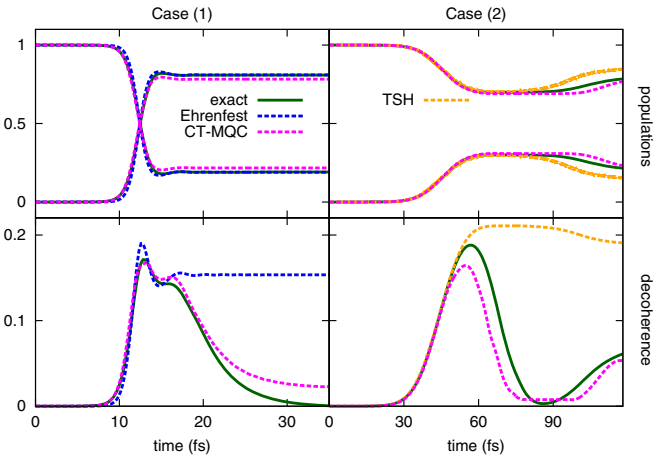

FIG. 3 (color online). Populations of the BO states (upper panels) and indicator of decoherence (lower panels) as functions of time for model case (1) (left) and model case (2) (right).

[1] D. Polli, P. Altoè, O. Weingart, K. M. Spillane, C. Manzoni, D. Brida, G. Tomasello, G. Orlandi, P. Kukura, R. A. Mathies, M. Garavelli, and G. Cerullo, Nature (London) **467**, 440 (2010); S. Hayashi, E. Tajkhorshid, and K. Schulten, Biophys. J. **96**, 403 (2009); W. C. Chung, S. Nanbu, and T. Ishida, J. Phys. Chem. B **116**, 8009 (2012).

[2] E. Tapavicza, A. M. Meyer, and F. Furche, Phys. Chem. Chem. Phys. **13**, 20986 (2011); T. Brixner, J. Stenger, H. M. Vaswani, M. Cho, R. E. Blankenship, and G. R. Fleming, Nature (London) **434**, 625 (2005).

[3] C. A. Rozzi, S. M. Falke, N. Spallanzani, A. Rubio, E. Molinari, D. Brida, M. Maiuri, G. Cerullo, H. Schramm, J. Christoffers, and C. Lienau, Nat. Commun. **4**, 1602 (2013); C. Silva, Nat. Mater. **12**, 5 (2013); A. E. Jailaubekov, A. P. Willard, J. R. Tritsch, W.-L. Chan, N. Sai, R. Gearba, L. G. Kaake, K. J. Williams, K. Leung, P. J. Rossky, and X.-Y. Zhu, Nat. Mater. **12**, 66 (2013).

[4] A. L. Sobolewski, W. Domcke, C. Dedonder-Lardeux, and C. Jouvet, Phys. Chem. Chem. Phys. **4**, 1093 (2002); M. T. do N. Varella, Y. Arasaki, H. Ushiyama, V. McKoy, and K. Takatsukas, J. Chem. Phys. **124**, 154302 (2006); J.-Y. Fang and S. Hammes-Schiffer, J. Chem. Phys. **107**, 8933 (1997); D. Marx, ChemPhysChem **7**, 1848 (2006).

[5] T. J. Martínez and R. D. Levine, Chem. Phys. Lett. **259**, 252 (1996); T. J. Martínez, M. Ben-Nun, and R. D. Levine, J. Phys. Chem. **100**, 7884 (1996); T. J. Martinez, Acc. Chem. Res. **39**, 119 (2006); H.-D. Meyer, U. Manthe, and L. S. Cederbaum, Chem. Phys. Lett. **165**, 73 (1990); I. Burghardt, H.-D. Meyer, and L. S. Cederbaum, J. Chem. Phys. **111**, 2927 (1999); H.-D. Meyer and G. A. Worth, Theor. Chem. Acc. **109**, 251 (2003); M. Thoss, W. Domcke, and H. Wang, Chem. Phys. **296**, 217 (2004); H. Wang and M. Thoss, J. Chem. Phys. **119**, 1289 (2003); J. Li, I. Kondov, H. Wang, and M. Thoss, J. Phys. Chem. C **114**, 18481 (2010); Q. Meng, S. Faraji, O. Vendrell, and H.-D. Meyer, J. Chem. Phys. **137**, 134302 (2012); M. Schröder, J.-L. Carreón-Macedo, and A. Brown, Phys. Chem. Chem. Phys. **10**, 850 (2008).

[6] P. Ehrenfest, Z. Phys. **45**, 455 (1927); D. V. Shalashilin, J. Chem. Phys. **130**, 244101 (2009); R. Kapral and G. Ciccotti, J. Chem. Phys. **110**, 8919 (1999); B. F. E. Curchod, I. Tavernelli, and U. Rothlisberger, Phys. Chem. Chem. Phys. **13**, 3231 (2011); S. Bonella and D. F. Coker, J. Chem. Phys. **122**, 194102 (2005); N. L. Doltsinis and D. Marx, Phys. Rev. Lett. **88**, 166402 (2002); P. Pechukas, Phys. Rev. **181**, 166 (1969); J. E. Subotnik, J. Chem. Phys. **132**, 134112 (2010); Y. Wu and M. Herman, J. Chem. Phys. **123**, 144106 (2005); D. F. Coker and L. Xiao, J. Chem. Phys. **102**, 496 (1995); O. V. Prezhdo and P. J. Rossky, J. Chem. Phys. **107**, 825 (1997); G. Stock and M. Thoss, Phys. Rev. Lett. **78**, 578 (1997); X. Sun and W. H. Miller, J. Chem. Phys. **106**, 6346 (1997); A. W. Jasper, C. Zhu, S. Nangia, and D. G. Truhlar, Faraday Discuss. **127**, 1 (2004); S. Nielsen, R. Kapral, and G. Ciccotti, J. Chem. Phys. **112**, 6543 (2000); C.-Y. Hsieh and R. Kapral, J. Chem. Phys. **138**, 134110 (2013); P. Huo and D. F. Coker, J. Chem. Phys. **137**, 22A535 (2012); R. E. Wyatt, C. L. Lopreore, and G. Parlant, J. Chem. Phys. **114**, 5113 (2001); I. Burghardt, J. Chem. Phys. **122**, 094103 (2005); O. V. Prezhdo and C. Brooksby, Phys. Rev. Lett. **86**, 3215 (2001); N. Zamstein and D. J. Tannor, J. Chem. Phys. **137**, 22A518 (2012); D. Bousquet, K. H. Hughes, D. A. Micha, and I. Burghardt, J. Chem. Phys. **134**, 064116 (2011); J. O. Richardson and M. Thoss, J. Chem. Phys. **139**, 031102 (2013); N. Ananth, J. Chem. Phys. **139**, 124102 (2013); F. Agostini, S. Caprara, and G. Ciccotti, Europhys. Lett. **78**, 30001 (2007).

[7] A. Abedi, F. Agostini, and E. K. U. Gross, Europhys. Lett. **106**, 33001 (2014).

[8] F. Agostini, A. Abedi, and E. K. U. Gross, J. Chem. Phys. **141**, 214101 (2014).

[9] J. C. Tully, J. Chem. Phys. **93**, 1061 (1990).

[10] J. E. Subotnik and N. Shenvi, J. Chem. Phys. **134**, 244114 (2011); B. R. Landry and J. E. Subotnik, J. Chem. Phys. **135**, 191101 (2011); J. E. Subotnik and N. Shenvi, J. Chem. Phys. **134**, 024105 (2011); N. Shenvi, J. E. Subotnik, and W. Yang, J. Chem. Phys. **135**, 024101 (2011); B. F. E. Curchod and I. Tavernelli, J. Chem. Phys. **138**, 184112 (2013); T. J. Penfold and G. A. Worth, J. Mol. Graphics Modell. **26**, 613 (2007); G. A. Worth, P. Hunt, and M. A. Robb, J. Phys. Chem. A **107**, 621 (2003); D. Kohen, F. H. Stillinger, and J. C. Tully, J. Chem. Phys. **109**, 4713 (1998).

[11] A. Abedi, N. T. Maitra, and E. K. U. Gross, Phys. Rev. Lett. **105**, 123002 (2010); J. Chem. Phys. **137**, 22A530 (2012); Y. Suzuki, A. Abedi, N. T. Maitra, and E. K. U. Gross, Phys. Rev. A **89**, 040501 (2014).

[12] It should be noted that, in addition to the scalar potential energy surface, there is, in the most general case, also a Berry-type vector potential, as is evident in Eqs. (2)–(4). In some cases, this vector potential may vanish identically [see S. K. Min, A. Abedi, K. S. Kim, and E. K. U. Gross, Phys. Rev. Lett. **113**, 263004 (2014)].

[13] A. Abedi, F. Agostini, Y. Suzuki, and E. K. U. Gross, Phys. Rev. Lett. **110**, 263001 (2013).

[14] F. Agostini, A. Abedi, Y. Suzuki, and E. K. U. Gross, Mol. Phys. **111**, 3625 (2013); F. Agostini, A. Abedi, Y. Suzuki, S. K. Min, N. T. Maitra, and E. K. U. Gross, J. Chem. Phys. **142**, 084303 (2015).

[15] F. Agostini, S. K. Min, and E. K. U. Gross, Ann. Phys. (N.Y.), doi:10.1002/andp.201500108.

[16] N. C. Handy, Y. Yamaguchi, and H. F. Schaefer III, J. Chem. Phys. **84**, 4481 (1986).

[17] E. F. Valeev and C. D. Sherrill, J. Chem. Phys. **118**, 3921 (2003).

[18] We note that $\Phi_{\underline{\underline{\mathbf{R}}}}(\underline{\underline{\mathbf{r}}}, t)$ may contain a translational phase like $e^{i\underline{\underline{\mathbf{K}}}\cdot\underline{\underline{\mathbf{R}}}}$, where $\underline{\underline{\mathbf{K}}}$ is the linear momentum associated to the motion of the nuclear system as a rigid body. The second derivative with respect to $\mathbf{R}_\nu$ then yields a term proportional to $\mathbf{K}_\nu^2$ which is proportional to M_ν^2. However, the vector potential in the neglected term of the TDPES contains a similar term which cancels out all M_ν^2 dependencies.

[19] J. C. Tully, in *Proceedings of the International School of Physics*, edited by B. B. Berne, G. Ciccotti, and D. F. Coker (World Scientific, Singapore, 1997).

[20] See Supplemental Material at http://link.aps.org/supplemental/10.1103/PhysRevLett.115.073001 for more computational details, which includes Ref. [21].

[21] M. D. Feit, F. A. Fleck, Jr., and A. Steiger, J. Comput. Phys. **47**, 412 (1982).

[22] S. K. Min, F. Agostini, and E. K. U. Gross (to be published).

[23] S. Shin and H. Metiu, J. Chem. Phys. **102**, 9285 (1995).

[24] J. E. Subotnik, W. Ouyang, and B. R. Landry, J. Chem. Phys. **139**, 214107 (2013).